BIOCHEMICAL PHARMACOLOGY 71 (2006) 779–790

available at www.sciencedirect.com

SCIENCE DIRECT®

journal homepage: www.elsevier.com/locate/biochempharm

Selective lysis of erythrocytes infected with the trophozoite stage of *Plasmodium falciparum* by polyene macrolide antibiotics

Ursula I.M. Wiehart [a], *Marina Rautenbach* [b], *Heinrich C. Hoppe* [a,*]

[a] *Division of Pharmacology and Institute of Infectious Diseases and Molecular Medicine, University of Cape Town, Medical School Observatory, 7925 Cape Town, South Africa*
[b] *Department of Biochemistry, University of Stellenbosch, South Africa*

ARTICLE INFO

Article history:
Received 28 September 2005
Accepted 14 December 2005

Keywords:
Malaria
Erythrocyte
Amphotericin
Nystatin
Filipin
Haemolysis

ABSTRACT

The continuous increase in strains of the human malaria parasite *Plasmodium falciparum* resistant to most front-line antimalarial compounds is reason for grave clinical concern. The search for new drugs led us to investigate a number of membrane active polyene macrolide antibiotics, such as amphotericin B, nystatin, filipin and natamycin. The interaction of these compounds with sterols in bilayer cell membranes can lead to cell damage and ultimately cell lysis. The malaria parasite modifies the host erythrocyte membrane by changing the protein and lipid composition and thus the infected cell could be a selective target for membrane active compounds. We found that erythrocytes infected with the trophozoite stage of *P. falciparum* were particularly susceptible to lysis by amphotericin B (Fungizone™) and, to a lesser extent, nystatin, as determined by ELISA and various microscopy assays. Liposomal amphotericin B (AmBisome™) displayed a similar specificity for parasitised erythrocytes, but complete lysis required a longer incubation period. In contrast, filipin and natamycin did not distinguish between normal and parasite-infected erythrocytes, but lysed both at similar concentrations. In addition, when added to ring-stage cultures, the amphotericin B preparations and nystatin produced a marked disruption in parasite morphology in less than 2 h without an accompanying permeabilisation of the infected host cell, suggesting a second plasmodicidal mode of action. The results imply that selected polyene macrolide antibiotics or their derivatives could find application in the treatment of severe malaria caused by of *P. falciparum*.

1. Introduction

Following the initial success of global control programs, malaria has resurged as the most devastating tropical disease in the latter part of the last century. Reasons for this are varied, but a major contributing factor is the rapid emergence and spread of parasite resistance to front-line drugs, which has provoked an urgent search for novel or improved antimalarial compounds [1]. The disease is caused by protozoans of the genus *Plasmodium* which are transmitted to humans by *Anopheles* mosquitoes. Following an asymptomatic period of growth and multiplication in liver cells, the parasites rupture into the circulation in the form of merozoites that rapidly invade erythrocytes. Immediately following invasion, the

* Corresponding author. Tel.: +27 21 406 6498; fax: +27 21 448 1989.
E-mail address: hhoppe@uctgsh1.uct.ac.za (H.C. Hoppe).
0006-2952/$ – see front matter © 2006 Elsevier Inc. All rights reserved.
doi:10.1016/j.bcp.2005.12.012

merozoite differentiates into a ring form that ingests erythrocyte cytoplasm and grows into a trophozoite. In the subsequent schizont stage growth ceases, the nucleus undergoes multiple divisions and the plasma membrane invaginates to give rise to several daughter merozoites that escape from the infected host cell and invade fresh erythrocytes. This cycle is completed every 48 h and is responsible for the pathology of malaria. Initial symptoms are varied and often described as ''flu-like'', but among the most life-threatening consequence of an infection by the most prevalent species, *Plasmodium falciparum*, is a condition known as cerebral malaria. Infected erythrocytes have an altered surface composition, including the presence of parasite proteins, which results in their aggregation and binding to non-infected cells to yield red blood cell clumps or rosettes [2]. In addition, binding of the rosettes to endothelial cells in brain capillaries and accompanying inflammatory responses can reduce perfusion in critical areas and contribute to the pathogenesis of cerebral malaria, leading to convulsions, coma and death of the infected individual [3,4].

During its residence inside the red blood cell, the parasite extensively customises the host cell to meet its requirements. Several parasite proteins associate with the erythrocyte membrane and contribute to rosetting [2,4]. To facilitate transport of the proteins to the membrane, the parasite constructs novel membrane-bound organelles in the erythrocyte cytoplasm [5] and the proteins may be delivered to the erythrocyte plasma membrane by vesicular trafficking [6,7]. Vesicular fusion conceivably alters the lipid composition and properties of the latter membrane. In addition to the secretory traffic, detergent resistant erythrocyte membrane lipid rafts and associated proteins are imported to the parasite, potentially further modifying the host membrane [8]. To acquire vital nutrients, the permeability of the erythrocyte membrane to low molecular weight compounds is increased [9], while neoantigens are created on the erythrocyte surface by the modification of native integral erythrocyte membrane proteins during parasite infection [10]. The result of these activities is an alteration of the membrane protein and lipid composition and distribution in erythrocytes infected with mature malaria parasites [11–16].

The parasite-induced modification of the infected red blood cell membrane raises the possibility that the latter may be vulnerable to selective recognition and perturbation by membrane active drugs and compounds. A group of antifungal compounds, mostly classified as polyene macrolides, are membranolytic due to their lipid (in particular sterol) binding activity. Natamycin (pimaricin) is used as a food preservative and in the treatment of fungal keratitis due to its ability to bind sterols and disrupt fungal membranes [17–19]. Amphotericin B (AmB) and nystatin are commonly used for the treatment of topical and systemic (in the case of the former) fungal infections and are thought to permeabilise target membranes by binding to β-ergosterol, the principal fungal sterol [19–23]. Toxicity problems encountered with AmB and nystatin are attributed to the ability of the polyene macrolides to also bind cholesterol in human cell membranes, albeit with a lower affinity, which has led to the development of liposomal formulations of the compounds for intravenous use [24–26]. Heat-treated AmB-deoxycholate has recently been reported to have activity against *P. falciparum* at low to sub-micromolar concentrations [27]. The polyene macrolide compound filipin is widely used in cell biological studies of cholesterol dynamics due to its affinity for cholesterol and its inherent fluorescent properties [28].

In this study we report the antimalarial activity and haemolytic selectivity of a number of polyene macrolides, namely: filipin, natamycin, AmB and nystatin. A sensitive ELISA (enzyme-linked immuno-sorbent assay) procedure was developed to compare the ability of the compounds to lyse trophozoite-infected vs. uninfected erythrocytes. The mechanism of action of the most selective compounds was further investigated in trophozoite and ring-infected cultures using light, fluorescence and electron microscopy assays.

2. Materials and methods

2.1. Drugs used in this study

Filipin complex from *Streptomyces filipinesis*, nystatin dihydrate, saponin and natamycin (pimaricin) were obtained from Sigma–Aldrich, an amphotericin B-deoxycholate preparation (Fungizone™) from Bristol-Myers Squibb and liposomal amphotericin B (AmBisome™) from Key Oncologics. Filipin and nystatin stock solutions were prepared in dimethyl sulfoxide (DMSO; 25 mg/ml and 10 mM, respectively) and stored frozen. Saponin was stored at 4 °C as a 50 mg/ml solution in water. Amphotericin B-deoxycholate was dissolved in water to 0.5 mM according to manufacturer's specifications and stored frozen. Liposomal amphotericin B was also reconstituted to 0.5 mM in water, according to manufacturer's specifications, immediately before use. Natamycin was dissolved in a minimum amount of acetic acid, diluted in culture medium and neutralised with NaOH to yield a 3 mM stock solution shortly before use.

2.2. Parasite culture

The D10 strain of *P. falciparum* was cultured in RPMI-1640 medium supplemented with 50 mM glucose, 0.65 mM hypoxanthine, 25 mM Hepes, 0.2% (w/v) $NaHCO_3$, 0.048 mg/ml gentamicin, 0.5% (w/v) Albumax II, and 2–4% (v/v) human O^+ erythrocytes, under an atmosphere of 3% CO_2, 4% O_2, balance N_2.

2.3. Parasite viability and haemolysis dose–response assays

Culture-derived parasitised erythrocytes were mixed with fresh culture medium and erythrocytes to yield a 2% parasitemia, 2% haematocrit suspension and distributed in microtitre plates at 90 μl/well. Serial dilutions of test drug in culture medium were prepared in quadruplicate wells in a separate plate and transferred to the parasite plate to yield a final volume of 100 μl/well. The plates were incubated at 37 °C for 48 h and parasite viability in each well measured by the colorimetric determination of lactate dehydrogenase activity [29].

To determine haemolytic activity of the drugs, parallel plates were prepared containing 90 μl/well of a 2% haematocrit suspension of uninfected erythrocytes and 10 μl/well of the serial drug dilutions was added. After the 48-h incubation, intact erythrocytes were sedimented in the microtitre plate wells by centrifugation at 200 × *g* for 3 min in a swing-out rotor. Aliquots of the supernatants were removed and diluted 1:8 in water in separate microtitre plates. Haemoglobin content in the supernatant dilutions was determined by absorbance at 405 nm in a microtitre plate spectrophotometer. Absorbance readings were converted to percentage haemolysis, or, in the case of the lactate dehydrogenase assays, to percentage parasite viability.

2.4. Data processing

All dose–response data was analysed using Graphpad Prism version 3.01 for Windows, (GraphPad Software, San Diego, California, USA). Non-linear regression was performed on the dose–response data obtained from the lactate dehydrogenase and haemolysis assays. A sigmoidal curve with variable slope and constant difference of 100 ± 5 between the top and bottom was fitted to each of the data sets using the following equation:

$$\%\,\text{growth inhibition} = Y = \frac{(\text{top} - \text{bottom})}{(1 + 10^{(\log \text{IC}_{50} - X)\text{Hill slope}})}$$

For curve fitting only the mean value of each data point, without weighting, was considered. The 50% inhibitory concentration (IC_{50}) was calculated from the *X*-value of the response halfway between top and bottom plateau. Experiments, with three to eight determinations at each concentration, were performed for each compound against each target cell. Between 30 and 80 data points were considered in each dose–response curve to calculate the IC_{50} (concentration that leads to 50% growth inhibition), and HC_{50} (concentration that leads to 50% erythrocyte lysis).

2.5. ELISA-based haemolysis assay

Parasite-infected erythrocytes (pRBC) were separated from uninfected erythrocytes by centrifugation through a step-wise Percoll gradient containing 3% alanine [30]. Serial dilutions of test drugs were added to suspensions of the enriched pRBC or uninfected erythrocytes in Albumax-free culture medium in microtitre plates (0.2% final hematocrit, 50 μl final volume/well). After a 40-min incubation at 37 °C, intact erythrocytes were sedimented by centrifugation at 200 × *g* for 3 min in a swing-out rotor. Aliquots of the supernatants were diluted 50 times in PBS, transferred to ELISA plates (50 μl/well) and incubated for 20 min at room temperature. The plates were washed in phosphate-buffered saline (PBS), blocked in PBS containing 1% (w/v) bovine serum albumin and 0.1% (v/v) Tween 20 (blocking buffer) for 20 min and incubated for an additional 20 min with rabbit anti-human haemoglobin antiserum (Sigma–Aldrich) diluted 1:2000 in blocking buffer. Following four washes in PBS-0.1% (v/v) Tween 20 (washing buffer), plates were incubated with peroxidase-conjugated goat anti-rabbit antiserum (KPL Laboratories) diluted 1:2000 in blocking buffer. Following washes in washing buffer, bound peroxidase activity was determined colorimetrically by adding 0.1 M phosphate–citrate buffer (pH 4.8) containing 1 mg/ml *o*-phenylenediamine and 0.015% H_2O_2. Colour development was terminated by adding 2.5N sulphuric acid and quantified by absorbance at 450 nm using a microtitre plate reader. Duplicate experiments with each measurement in triplicate were performed to determine the HC_{50}-values from dose–response curves (analysed as described above). Selectivity was calculated from the ratio between the minimum concentration of each compound causing 100 ± 5% lysis (HC_{100}) of infected and uninfected cells (Selectivity = HC_{100} (normal cells)/HC_{100} (infected cells)).

2.6. Light microscopy

Drugs were added to parasite cultures (2% haematocrit) and incubated at 37 °C. At various time-points, blood smears were prepared on microscope slides, stained with Giemsa solution and viewed by light microscopy. Alternatively, aliquots were removed from the cultures, directly mounted on microscope slides under glass cover slips and examined by phase-contrast light microscopy. For fluorescence microscopy analysis, aliquots removed from the drug-treated cultures were mixed with a solution of trypan blue and 4′,6-diamidino-2-phenylindole (DAPI) in PBS (final concentrations 0.5% and 1 μg/ml, respectively), mounted on microscope slides under cover slips and viewed by epifluorescence illumination using tetramethyl-rhodamine and ultraviolet filters. Alternatively, for the analysis of ring-stage parasite morphology following drug treatment, erythrocytes from treated cultures were centrifuged through 60% Percoll in RPMI medium for 10 min to remove lysed cells and debris, immobilized on poly-lysine-coated glass cover slips, rinsed in 0.5 mg/ml saponin in PBS and fixed for 10 min in PBS containing 3% paraformaldehyde and 0.2% glutaraldehyde. Cover slips were subsequently incubated for 5 min in PBS containing DAPI and trypan blue, inverted on microscope slides and viewed by fluorescence microscopy. All microscopy assays were performed on a Nikon Eclipse E600 fluorescence microscope fitted with a 100× Apochromat objective and images were captured with a Media Cybernetics CoolSNAP-Pro monochrome cooled CCD camera.

2.7. Electron microscopy

Parasite cultures were treated with 1.3 μM AmB for 30 min (trophozoite-stage cultures) or 70 min (ring-stage cultures). Treated cells were subsequently sedimented by centrifugation at 4000 × *g* for 3 min, washed in cacodylate buffer (0.1 M sodium cacodylate, 0.1 M sucrose, 2 mM $CaCl_2$, 2 mM $MgCl_2$, pH 7.2) and fixed in cacodylate buffer containing 2% paraformaldehyde and 2.5% glutaraldehyde for 1 h. After washing, fixed cells were incubated for 1 h in cacodylate buffer containing 1% tannic acid, washed, and post-fixed in 1% osmium tetroxide for an additional hour. Fixed cells were dehydrated by incubation in increasing concentrations of ethanol, transferred to acetone and embedded in Spurr's resin. Ultrathin sections were stained with uranyl acetate and lead citrate and viewed with a Jeol 1200 EX2 transmission electron microscope.

3. Results

3.1. Determination of parasite-inhibitory and haemolytic concentrations

The antimalarial activity of formulations of the polyene macrolides filipin (complex from *S. filipinensis*), natamycin (pimaricin), nystatin (nystatin dihydrate), AmB (amphotericin B-deoxycholate; Fungizone™) and liposomal AmB (AmBisome™) was determined by 48-h incubation of parasite cultures with serial dilutions of the compounds. Parasite viability was assessed by a colorimetric assay for parasite lactate dehydrogenase activity. Given that the parasites invade and grow in erythrocytes and that the polyene macrolides are haemolytic at high concentrations, haemolytic activity of the compounds was tested in parallel by spectrophotometrically measuring haemoglobin release from uninfected erythrocytes incubated under identical conditions. Since polyene macrolides disrupt membranes by interaction with sterols, the cholesterol-binding and haemolytic agent saponin was also tested. As shown in Fig. 1A–C, the concentrations that yielded 50% parasite inhibition (IC_{50})

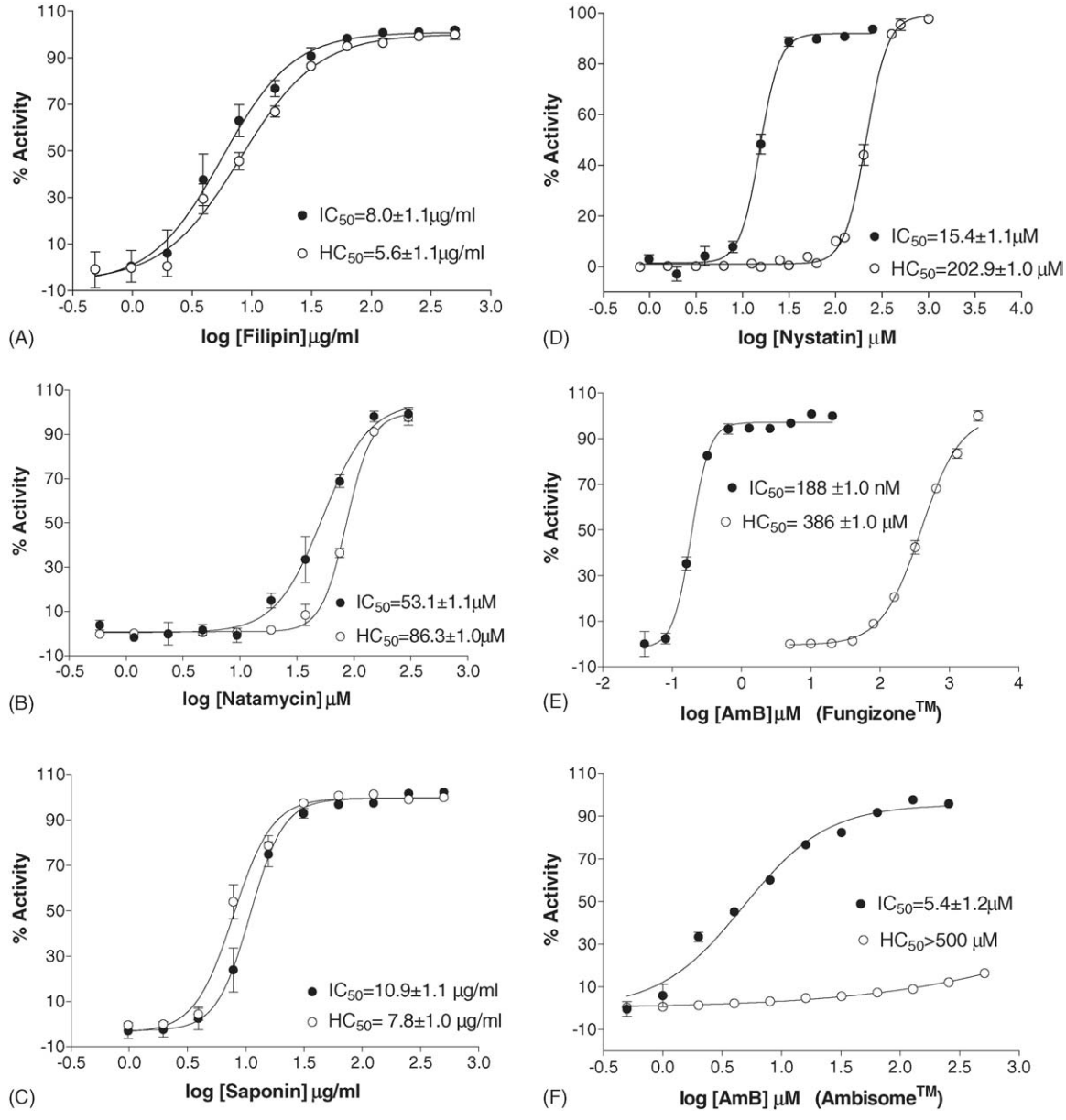

Fig. 1 – Growth inhibition dose–responses, obtained with trophozoite-infected erythrocytes (filled circles) and haemolytic dose–responses of normal erythrocytes (unfilled circles) as measured after 48 h. Growth inhibition was determined by a colorimetric lactase dehydrogenase assay and haemolysis of normal erythrocytes by measuring the released haemoglobin in the supernatant at 412 nm. Cells were treated with serial dilutions of filipin (A), natamycin (B), saponin (C) nystatin (D), amphotericin B (E) or liposomal amphotericin B (F). The average of at least three determinations of each data point ± standard error of the mean (SEM) is shown. Between 30 and 80 data points were used to generate the sigmoidal dose–response curves from which the HC_{50} and IC_{50} values were calculated.

and haemolysis (HC_{50}) were similar in the cases of filipin, saponin and natamycin, indicating that these compounds inhibit parasite viability by a general lysis of erythrocytes. In contrast, the IC_{50} s obtained with nystatin (IC_{50} = 15.4 μM) and especially AmB (IC_{50} = 0.188 μM) were markedly lower than their HC_{50} s (202.9 and 386 μM, respectively; Fig. 1D and E). Similarly, liposomal AmB yielded a distinctly increased anti-parasitic activity compared to normal erythrocyte lysis (Fig. 1F). The IC_{50} obtained with liposomal AmB was 5.4 μM, while a maximum erythrocyte lysis of only 15% was found over the concentration range tested (0.5–511 μM). The observed differences between haemolysis and growth inhibition for nystatin and the AmB preparations indicate a parasite-inhibitory mechanism different from non-specific erythrocyte lysis.

3.2. *Evaluation of treated cultures by Giemsa-stained blood smears*

In order to gauge the effect of nystatin, AmB and liposomal AmB on cultured parasites and assess their modes of action, parasite cultures were incubated with the drugs at non-haemolytic concentrations 3–9-fold above compound IC_{50} s and Giemsa-stained blood smears were prepared at various time-points for evaluation by light microscopy. With trophozoite-infected cultures, 25-min incubations with nystatin and AmB caused most of the parasites to appear free of their host erythrocytes but otherwise morphologically indistinguishable from untreated trophozoites (Fig. 2A and C). Consequently, parasitemia (defined as the percentage of intact erythrocytes containing parasites) decreased significantly, with 50 μM nystatin leading to a 92% and 1.3 μM AmB to a 97% reduction within 60 min (Fig. 2, graph insert). Treatment with 51 μM liposomal AmB had a similar effect, however, the appearance of significant numbers of red blood cell-free trophozoites required much longer incubation times (not shown). Thirteen percent of the trophozoites in the culture appeared to be released from their host erythrocytes after 2 h and 35% after 9 h, resulting in a concomitant parasitemia decrease from 3.4% (at time 0) to 2.3% (after 9 h). As with nystatin and AmB, the extra-cellular parasites appeared morphologically intact. In addition, the trophozoites still contained in erythrocytes developed normally in the presence of the liposomal AmB, entering the schizont stage and completing merozoite formation and subsequent invasion of erythrocytes to yield ring-stage parasites after 21 h at 3.3% parasitemia, compared to 8.5% for untreated cultures.

The same concentrations of nystatin, AmB and liposomal AmB were also used to assess the effect of the compounds on ring-stage cultures by light microscopy of Giemsa-stained blood smears. In the case of both nystatin and AmB, no apparent red blood cell-free parasites were visible over a 2-h treatment time (Fig. 2D–F). However, a gradual decrease in parasitemia was observed (60% reduction with nystatin and 63% with AmB after 60 min; Fig. 2, graph insert). In addition, although the remaining rings were present in seemingly intact erythrocytes, their morphology had deteriorated. Following nystatin treatment, rings appeared more insubstantial and often had unusual structures (Fig. 2E), compared to control cultures (Fig. 2D), while AmB-treated rings were pyknotic

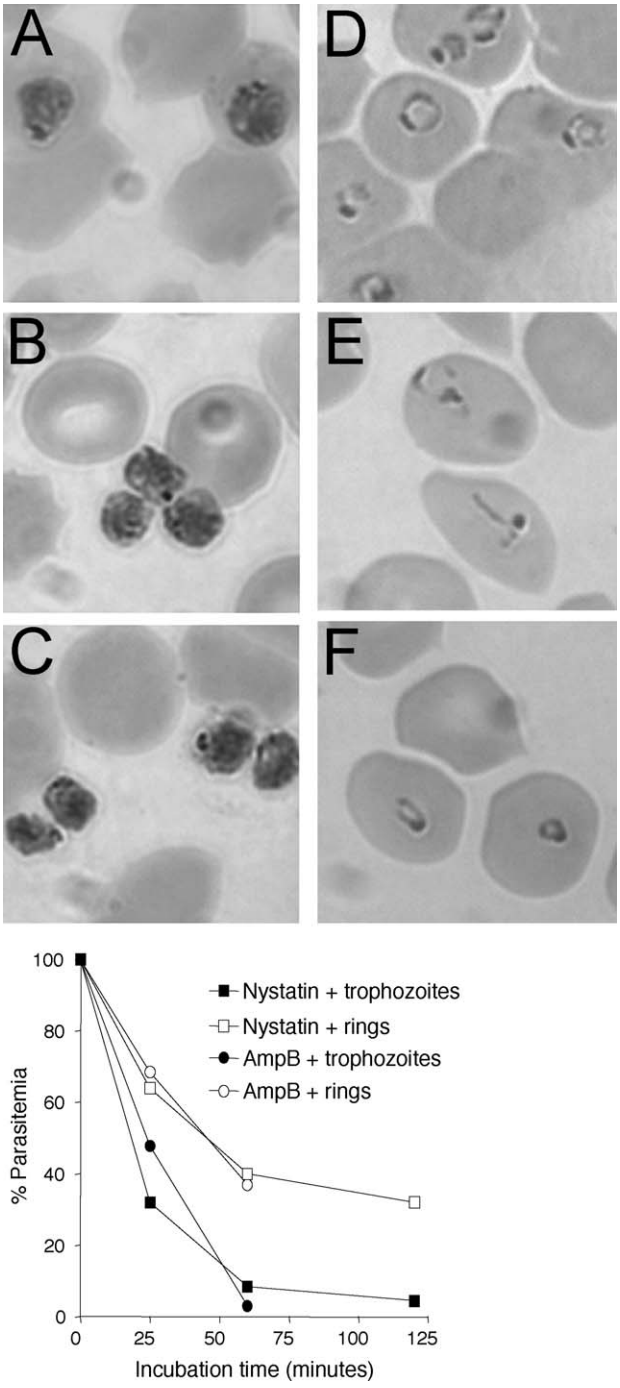

Fig. 2 – Giemsa-stained blood smears of treated cultures. Parasite cultures were left untreated (A and D), or incubated for 2 h with 50 μM nystatin (B and E) or 1.3 μM amphotericin B (C and F); (A–C) trophozoite-infected cultures; (D–F) ring-infected cultures. The graph inset shows the percentage parasitemia at various time-points during incubation of trophozoite (filled symbols) or ring-stage (open symbols) cultures with nystatin (squares) and AmB (circles).

(Fig. 2F). Liposomal AmB, by contrast, did not alter ring morphology or decrease parasitemia (results not shown) during 9 h of incubation. However, the rings failed to develop into trophozoites and after 21 h no parasites were visible in the

culture, while untreated cultures contained normally developed trophozoites.

3.3. *Evaluation of treated cultures by phase-contrast light microscopy*

The results obtained with the Giemsa-stained smears suggested that nystatin and AmB exert their anti-parasitic activity at sub-haemolytic concentrations by specifically lysing erythrocytes infected with trophozoites. However, cell membranes are not detectable in stained smears and the process of preparing the thin blood smears, fixing in methanol and Giemsa staining may disrupt fragile cells. We therefore assessed the effect of nystatin and AmB on trophozoite-infected cells at various time-points by directly mounting treated cultures under coverslips and immediately viewing the cells by phase-contrast microscopy. Treated cultures contained a mixture of trophozoites inside intact erythrocytes, trophozoites in lysed erythrocytes but surrounded by an erythrocyte ghost membrane and ''free'' trophozoites with no discernable surrounding host membrane (Fig. 3). During a 40-min incubation with 50 μM nystatin, there was a decrease in the percentage of parasites contained in intact erythrocytes and a concomitant increase in parasites in erythrocyte ghosts and free parasites (Fig. 3A). After 40 min, 67% of the parasites were located in lysed red blood cell ghosts and 25% were free of visible erythrocyte membranes. The same trend was observed by incubating parasite cultures in 1.3 μM AmB, except that

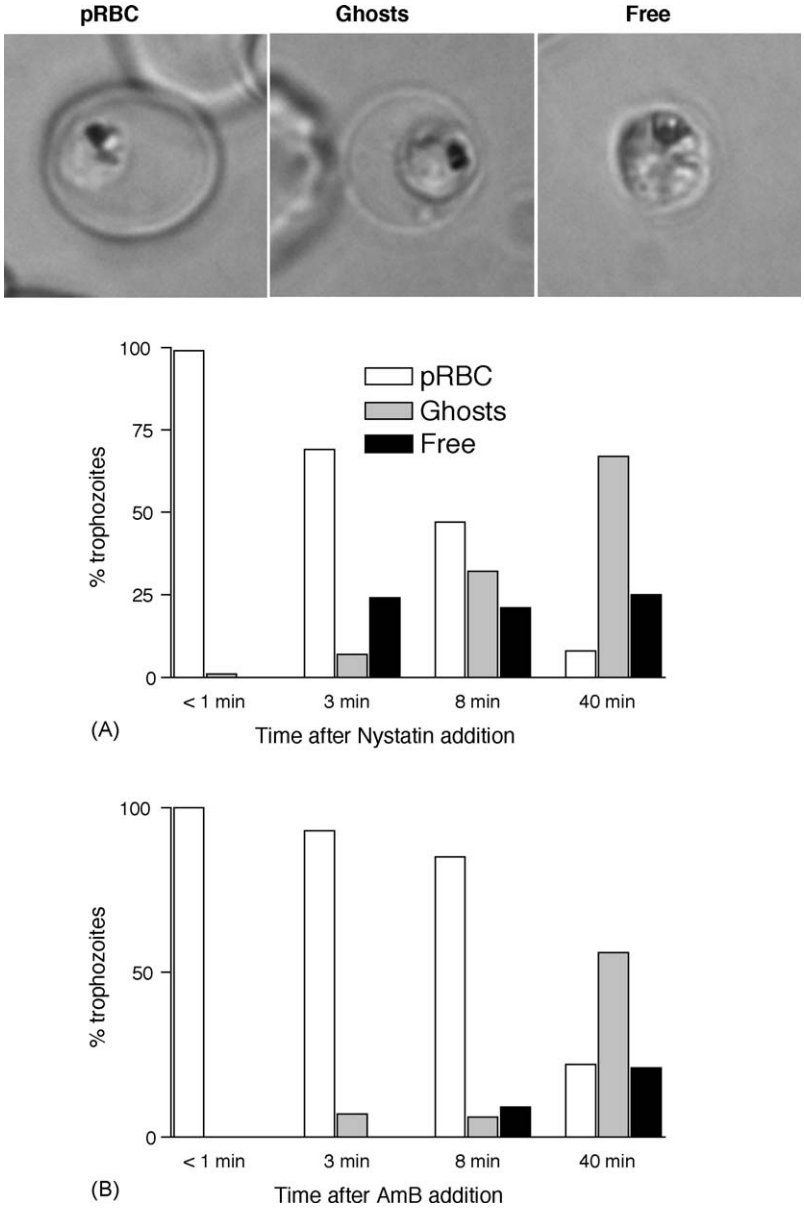

Fig. 3 – Phase-contrast microscopy of trophozoite-stage cultures. Cultures were incubated with 50 μM nystatin (A) or 1.3 μM amphotericin B (B) and the percentage of parasites found inside intact parasitised erythrocytes (pRBC; white bars), surrounded by a red blood cell ghost membrane (ghosts; grey bars), or free of surrounding host membranes (free; black bars), was determined at various time-points. Representative phase-contrast microscopy images of the three conditions are shown above the graphs.

erythrocyte lysis was more gradual (Fig. 3B). Uninfected erythrocytes appeared normal at all time-points.

3.4. Determination of haemolytic activity by ELISA

The results obtained with the light microscopy studies suggested that nystatin and AmB have the ability to selectively lyse trophozoite-infected erythrocytes. To allow the direct comparison of the dose-dependent haemolysis of trophozoite-infected versus uninfected erythrocytes, we developed a sensitive ELISA-based haemolysis assay. Trophozoite-infected erythrocytes isolated from parasite cultures by density centrifugation, as well as uninfected erythrocytes were incubated in serial dilutions of the test compounds for 40 min and haemoglobin released into the supernatant was detected with anti-haemoglobin antiserum (Table 1). The results showed the same trend as that found previously by comparing haemolytic activity (assessed by spectrophotometric detection of released haemoglobin) and parasite-inhibitory activity (compare Fig. 1 and Table 1). Filipin, natamycin and saponin were virtually unselective and did not distinguish between uninfected and parasitised erythrocytes (Table 1). Nystatin again showed an intermediate haemolytic selectivity (5-fold), while AmB lysed parasitised erythrocytes at low micromolar concentrations 65-fold lower than required for 100% haemolysis of normal erythrocytes (Table 1). The results indicate that the selective lysis of infected erythrocytes forms the basis of the anti-parasitic mechanism of action of AmB and nystatin in trophozoite-infected cultures. In the case of liposomal AmB, no detectable haemolysis was obtained over the concentration range used during the 40-min incubation with both uninfected and parasitised erythrocytes (results not shown). This agrees with the results obtained by light microscopic evaluation of liposomal AmB-treated cultures by Giemsa-stained blood smears in which a low percentage of red blood cell-free trophozoites were observed only after incubations of 2 h or longer.

3.5. Evaluation of parasite morphology by trypan blue fluorescence microscopy

As described above, the Giemsa-stained blood smears and light microscopic analysis of parasite cultures treated with nystatin and AmB suggested that these compounds lyse the plasma membranes of trophozoite-infected erythrocytes, but leave the parasites relatively intact (Fig. 2B and C, Fig. 3 phase-contrast images). To evaluate the membrane integrity of trophozoites following nystatin and AmB treatment, a trypan blue exclusion assay was performed. Parasite cultures were treated with 50 μM nystatin and 1.3 μM AmB for 40 min, suspended in a trypan blue solution and viewed by fluorescence microscopy. Using TRITC excitation filters, trypan blue yields a bright red fluorescence. In control cultures (Fig. 4A), trypan blue was bound to the erythrocyte plasma membrane (arrowhead). In addition, the increased permeability of erythrocytes infected with mature stage parasites to diverse low molecular weight compounds [31] resulted in trypan blue entering the red blood cell. Here it also bound to parasite-derived membranous organelles in the erythrocyte cytoplasm (Fig. 4A, small arrow) and to the parasite plasma membrane (Fig. 4A, large arrow). No conspicuous trypan blue staining of internal parasite structures was found. In nystatin-treated cultures, parasites were surrounded by a lysed red blood cell ghost membrane (Fig. 4B, right panel), which also bound trypan blue (Fig. 4B, arrowhead). Although the parasite plasma membrane was brightly stained with trypan blue (Fig. 4B, arrow), no trypan blue fluorescence was visible inside the parasite, suggesting that the integrity of the parasite plasma membrane was retained. Similar results were obtained with AmB-treated cultures (Fig. 4C). As a positive control for parasite membrane disruption, cultures were treated with 8 μM gramicidin S (Fig. 4D). In addition to staining the red blood cell ghost membrane (arrowhead), trypan blue was also found inside the parasite cytoplasm where it showed discernable labelling of internal parasite structures, including the nuclear membrane (small arrow) and around the haemozoin crystal (large arrow).

Trypan blue exclusion was also used to determine the effect of nystatin and AmB on erythrocyte membrane permeability in ring-stage cultures. In contrast to trophozoite-infected cells, ring-infected erythrocyte membranes largely retain their native impermeability to small molecules. Consequently, trypan blue brightly stained the red blood cell membranes in control cultures, but failed to penetrate this barrier and stain the parasite membrane or parasite-derived structures (not shown). Identical results were obtained with ring-stage cultures treated for 90 min with nystatin or AmB (the latter is shown in Fig. 4E), suggesting that these compounds do not significantly disrupt ring-infected erythrocyte permeability.

Giemsa-stained blood smears suggested that nystatin and AmB alter ring shapes following 1–2 h of incubation (Fig. 1E and F). Since stained smears inaccurately reflect ring structure, a modified trypan blue fluorescence microscopy

Table 1 – Summary of the dose-dependent hemolysis of normal vs. trophozoite-infected erythrocytes, as determined by ELISA

Compound	Trophozoite-infected erythrocytes	Erythrocytes	Selectivity
Fillipin	4 μg/ml	2 μg/ml	0.5
Nystatin	50 μM	250 μM	5
Natamycin	188 μM	188 μM	1
Amphotericin B-deoxycholate	2 μM	129 μM	65
Saponin	8 μg/ml	8 μg/ml	1

The concentrations given are the minimum concentration for each compound needed to cause 100 ± 5% haemolysis (HC_{100}). Selectivity is defined as HC_{100} (normal cells)/HC_{100} (infected cells).

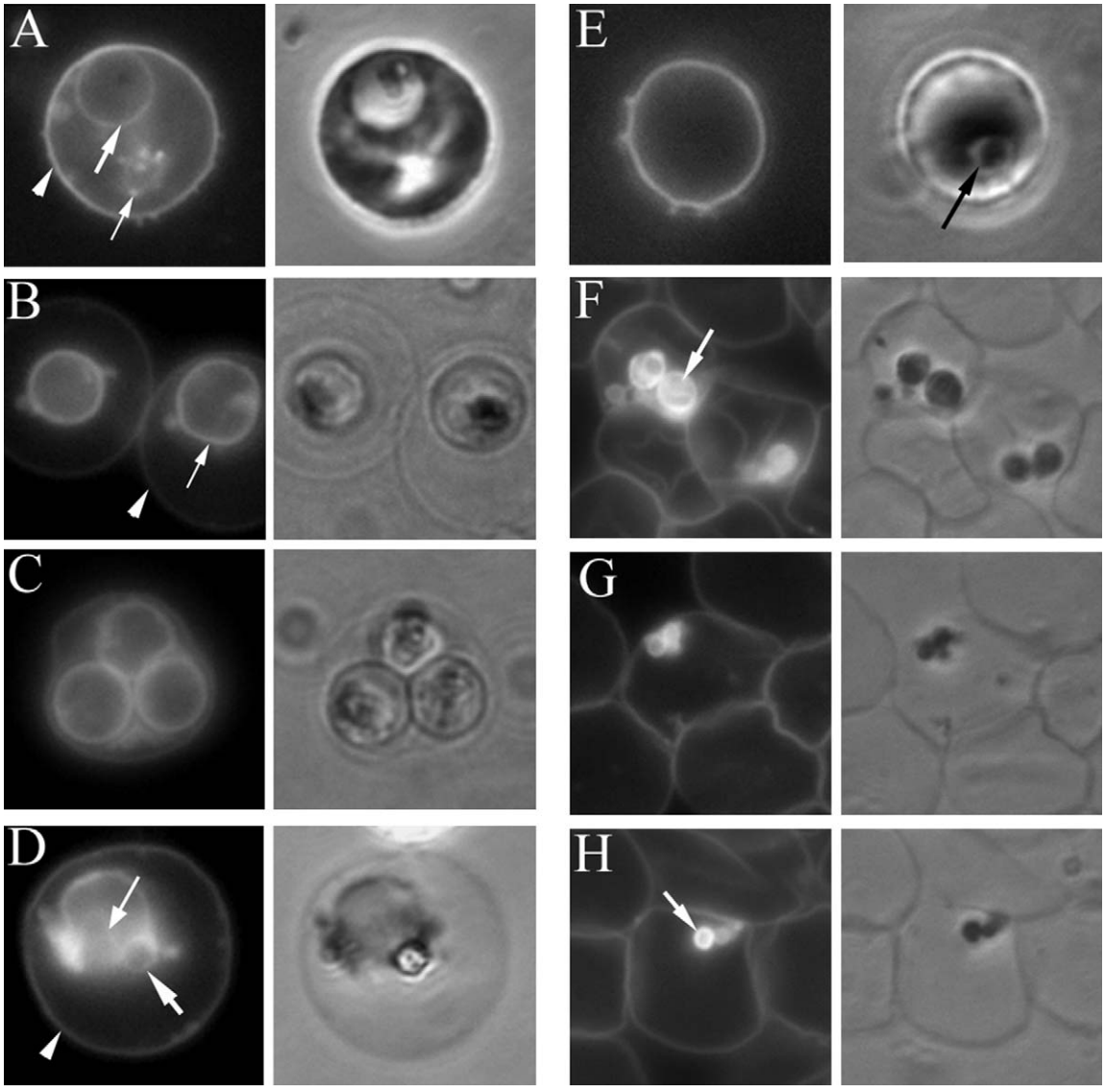

Fig. 4 – Fluorescence microscopy of drug-treated cultures incubated with trypan blue. Trophozoite-infected cultures were left untreated (A), or incubated with 50 μM nystatin (B), 1.3 μM amphotericin B (C) or 8 μM gramicidin S (D), resuspended in PBS containing trypan blue and viewed by fluorescence microscopy. In (A) arrowhead indicates trypan blue staining of the red blood cell membrane; small arrow, parasite-derived organelles in red blood cell cytoplasm; larger arrow, parasite plasma membrane. (B) Arrowhead indicates red blood cell ghost membrane; arrow, parasite plasma membrane. (D) Arrowhead indicates staining of the erythrocyte ghost membrane; larger arrow, accumulation of trypan blue around the hemozoin crystal; smaller arrow, staining of the nuclear membrane. Ring-infected cultures were also left untreated (F), or incubated for 2 h with amphotericin B (E and H) or nystatin (G). Following incubation, erythrocytes were either resuspended in trypan blue and viewed directly (E), or resuspended in trypan blue following aldehyde fixation and rinsing in saponin (F–H). In (E), the red blood cell membrane is strongly stained with trypan blue, but the dye has failed to penetrate the erythrocyte and stain the intracellular ring-stage parasite (denoted by the arrow in the phase-contrast image). In (F), the arrow indicates control, untreated ring-stage parasites surrounded by red blood cell ghost membranes. In (H), the arrow indicates the nuclear remnant of a pyknotic, amphotericin B-treated ring. In each case, the left-hand panel presents the fluorescence microscopy image and the right-hand panel the corresponding phase-contrast microscopy image.

assay was used to further assess the effect of these compounds on ring morphology following a 90-min incubation. Erythrocytes from treated cultures were centrifuged through Percoll to remove lysed cells and debris, immobilized on glass cover slips, briefly rinsed in saponin to lyse erythrocyte membranes and remove excess haemoglobin, fixed in paraformaldehyde/glutaraldehyde, immersed in trypan blue and viewed by fluorescence microscopy. In contrast to the well defined, rounded rings in control cells (Fig. 4F, arrow), fixed and permeabilised erythrocytes from nystatin-treated cultures contained irregularly shaped parasites considerably reduced in size (Fig. 4G). AmB-treated rings

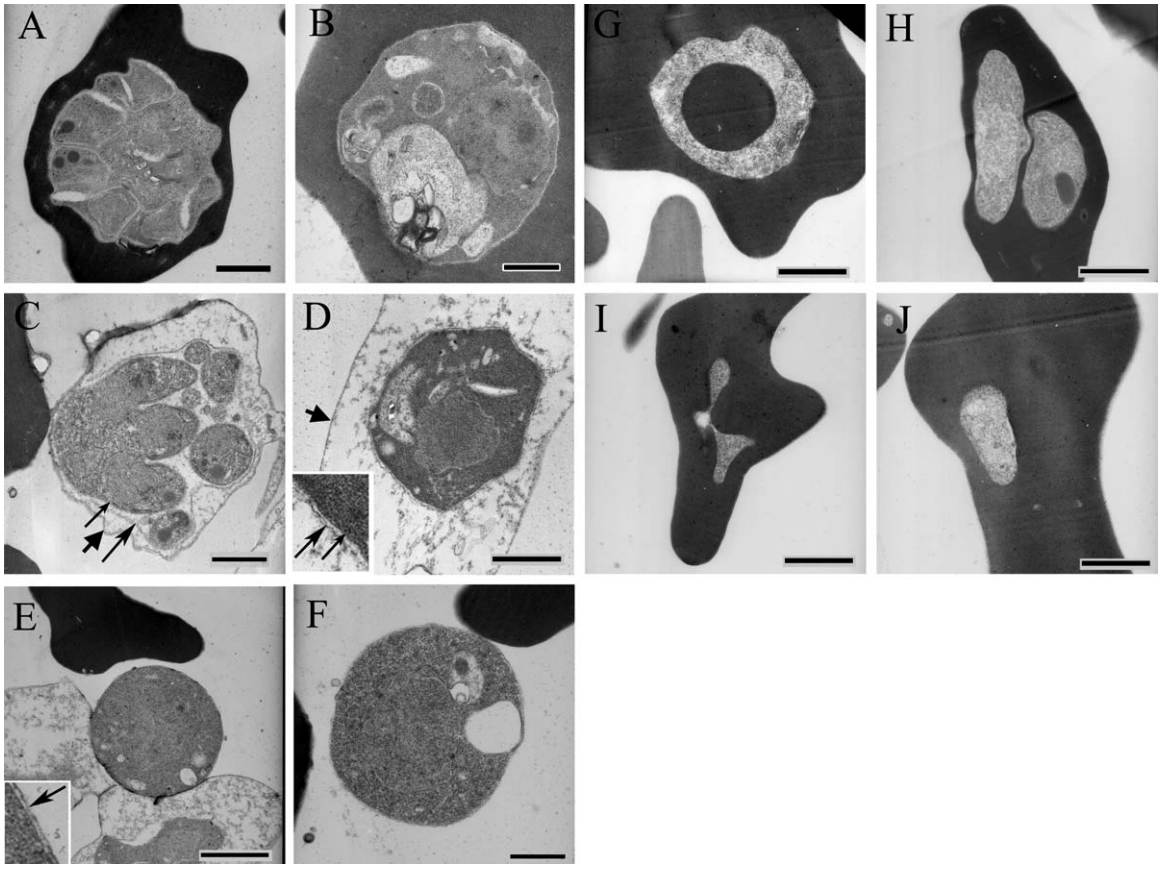

Fig. 5 – Transmission electron microscopy of AmB-treated cultures. (A and B) Untreated control schizont (A) and trophozoite (B) stage parasites in intact erythrocytes. (C and D) AmB-treated schizont (C) and trophozoite (D) surrounded by erythrocyte ghost membranes (arrowheads). Large arrows denote the parasitophorous vacuole membrane adjacent to the parasite membrane (latter indicated by small arrows). (E and F) AmB-treated trophozoites free of surrounding erythrocyte membranes. In (E), the free trophozoite is adjacent to an intact uninfected erythrocyte (top) and two lysed erythrocyte ghosts containing trophozoites. Arrow in inset indicates the parasitophorous vacuole membrane. (G and H) Untreated, control erythrocytes containing ring-stage parasites. (I and J) AmB-treated rings. The scale bars represent 1.0 μm in each case.

were reduced to the nucleus (Fig. 4H, arrow; discernable by DAPI staining not shown in these images) and a few membrane remnants.

3.6. *Evaluation of parasite morphology by transmission electron microscopy*

Examination of AmB-treated cultures by transmission electron microscopy (Fig. 5) confirmed the conclusions obtained by the phase-contrast and fluorescence microscopy experiments described above. After 30 min of treatment, cultures infected with mature parasites (trophozoites and schizonts) contained a mixture of parasites in unlysed erythrocytes similar to controls (Fig. 5A and B), intact parasites in erythrocyte ghosts (Fig. 5C and D) and parasites free of surrounding erythrocyte membranes (Fig. 5E and F). Fig. 5E demonstrates a ''free'' trophozoite abutting two trophozoite-containing ghosts and an unlysed uninfected erythrocyte. Upon closer examination, free and ghost-enclosed trophozoites and schizonts were found to retain an intact parasitophorous vacuole membrane in close apposition to the parasite plasma membrane (large arrows — Fig. 5C–E insets). Treated parasite cytoplasm density was similar to that of the controls and no consistent organellar abnormalities were found. AmB-treated ring-stage parasites were retained in intact, unlysed erythrocytes (Fig. 5I and J). No clear evidence of ring lysis was found, however, treated rings were generally reduced in size, consistent with the pyknotic rings seen in Giemsa-stained smears, and occasionally displayed unusual shapes (Fig. 5I). The distinctive ring profile obtained in horizontal cross-sections of control parasites (Fig. 5G) was not observed in treated samples.

4. Discussion

In this study we have investigated the possibility that the modifications wrought on erythrocytes by infecting malaria parasites renders the host cell membrane vulnerable to specific lysis by membrane active agents. We have focused on several polyene macrolide formulations, since these compounds have membrane permeabilising activity, are widely used in cell biological studies, are clinically important in treating topical and systemic fungal infections and have been reported to have plasmodicidal properties. Using a

sensitive ELISA haemolysis assay we found that AmB and, to a lesser extent, nystatin, permeabilise trophozoite-infected erythrocytes at concentrations significantly below those required for normal erythrocytes. The selective lysis of infected cells by these two preparations was further confirmed by Giemsa-stained blood smears and direct phase-contrast light microscopy. The results demonstrate that the specific haemolysis of trophozoite-infected erythrocytes contributes significantly to the plasmodicidal activity of the nystatin and AmB preparations.

The molecular basis for the lytic selectivity of AmB and nystatin is uncertain. A simple possibility might be that alterations or damage caused by infecting parasites renders erythrocyte membranes more fragile and innately labile when challenged with membrane active agents. However, an argument against this explanation is the finding that virtually identical concentrations were required to lyse both uninfected and trophozoite-infected erythrocytes in the case of filipin, saponin and natamycin. In addition, parasite-inhibitory and erythrolytic concentrations obtained with AmB and nystatin were comparable in D10 and 3D7 strain cultures, despite the altered mechanical properties and membrane rigidity caused by the presence of erythrocyte membrane knobs in cells infected with the latter strain [32].

Polyene macrolides have a known affinity for cholesterol and other sterols and binding to β-ergosterol in fungal membranes mediates the activity of nystatin and AmB [17–19,21–23]. However, the inability of the cholesterol-specific compounds saponin and filipin to distinguish haemolytically between infected and uninfected erythrocytes suggests that cholesterol binding per se may not explain the selectivity of nystatin and AmB. Of note is that AmB has been reported to have an enhanced affinity for oxidized forms of cholesterol [33]. Conceivably, the presence of oxidised cholesterol moieties in the infected erythrocyte membrane, caused by parasite-induced oxidation [34,35], could allow AmB and possibly nystatin to discriminate between infected and normal cells. In addition, the cholesterol-rich lipid rafts found in erythrocyte membranes appear to be disrupted during parasite infection, likely due to the reduction in cholesterol and sphingomyelin levels [15,36], which could result in an altered distribution and organization of cholesterol in the lipid bilayer and enhance nystatin or AmB-mediated permeabilisation. The latter may be further enhanced by the altered phospholipid bilayer distribution and composition of the infected erythrocyte membrane [13]. Noteworthy in this regard is the fact that the trophozoites themselves seem not to be significantly compromised by the AmB and nystatin concentrations that lyse infected host cells, correlating with the reported low cholesterol levels in parasite membranes [16,37]. Following treatment, the parasites appear morphologically intact in Giemsa-stained smears and by phase-contrast microscopy and remain impermeable to trypan blue. This suggests that the molecular target of the polyene macrolides in the infected erythrocyte membrane is not significantly present in trophozoite plasma membranes. The possibility remains that a non-sterol parasite-derived lipid/protein modification of the erythrocyte membrane forms the basis of AmB and nystatin selectivity.

In addition to the lysis of trophozoite-infected cells, our results indicate a second mode of action that contributes to the plasmodicidal activity of the nystatin and AmB preparations during the ring stage of the parasite life cycle. Ring morphology degenerated significantly after 1–2 h of treatment as judged by Giemsa-stained smears and by trypan blue membrane staining and fluorescence microscopy. This agrees with a recent report that suggested ring-stage parasites as the predominant target of heat-induced aggregates of AmB [27]. However, the rings were present in erythrocytes that appeared intact in blood smears, by light microscopy and trypan blue exclusion. This suggests that the polyene macrolide preparations do not destroy the ring-stage parasites by outright lysis of the infected erythrocytes, in contrast to what was found with trophozoite-infected cells. Conceivably, ring-infected host cell membranes have not yet accumulated the modifications required for selective lysis. Alternatively, AmB and nystatin may permeabilise the ring-infected erythrocyte membranes to an extent that does not result in haemoglobin release, but is sufficient to disrupt ion gradients and small molecule homeostasis and affect ring development and survival. The inability of trypan blue to penetrate ring-infected erythrocytes after 90 min of incubation with the polyene macrolide preparations, however, implies that this permeabilisation, if present, is not extensive. It has been reported that ring-stage parasites import and accumulate cholesterol-rich red blood cell membrane lipid rafts [8,38]. This produces an avenue by which AmB and nystatin may bind to raft cholesterol on the red blood cell surface, find their way to ring membranes and disrupt the latter. Such a mechanism would imply that ring-stage parasite membranes are significantly more prone to disruption by AmB and nystatin than later trophozoite membranes or uninfected red blood cell membranes, since both of the latter remain intact during treatment.

The liposomal AmB preparation, AmBisome^{TM}, appeared to have a plasmodicidal mode of action similar to that of nystatin and non-liposomal AmB, although considerably longer incubation times were required. A significant number of apparent red blood cell-free trophozoites were found after 9 h of incubation, as opposed to 30 min for nystatin and AmB. In fact, a number of trophozoites continued development into the schizont stage and completed subsequent invasion, yielding rings. Ring-stage parasite morphology or parasitemia was not affected over a 9 h period, compared to the considerable effects found with the other two macrolide preparations in 2 h or less, but the rings failed to develop into trophozoites.

The parasite-inhibitory concentration found for the AmB preparation in this study (188 nM) agrees with the IC_{50S} reported elsewhere [27] and also falls within the peak plasma concentration range obtained in clinical applications (0.5–2.2 μM; Fungizone package insert [http://home.intekom.com/pharm/bm_squib/fungiz-i.html]). Although the current intravenous route of AmB administration and toxic side effects make it a less than ideal therapeutic compound clinically, the rapid lysis of trophozoite-infected erythrocytes by AmB could conceivably rapidly destabilise obstructing rosettes responsible for severe and cerebral malaria and facilitate the restoration of perfusion to ischemic areas. In summary, this study highlights the capacity of membrane active compounds to selectively lyse malaria parasite-infected erythrocytes, with potential clinical

application in cases of severe malaria caused by sequestration of *Plasmodium falciparum*-infected cells.

Acknowledgement

The work presented here was funded by a Wellcome Trust Senior International Research Fellowship award to HCH.

REFERENCES

[1] Macreadie I, Ginsburg H, Sirawaraporn W, Tilley L. Antimalarial drug development and new targets. Parasitol Today 2000;16:438–44.
[2] Craig A, Scherf A. Molecules on the surface of the *Plasmodium falciparum* infected erythrocyte and their role in malaria pathogenesis and immune evasion. Mol Biochem Parasitol 2001;115:129–43.
[3] Adams S, Brown H, Turner G. Breaking down the blood-brain barrier: signalling a path to cerebral malaria? Trends Parasitol 2002;18:360–6.
[4] Sherman IW, Eda S, Winograd E. Cytoadherence and sequestration in *Plasmodium falciparum*: defining the ties that bind. Microbes Infect 2003;5:897–909.
[5] Przyborski JM, Wickert H, Krohne G, Lanzer M. Maurer's clefts — a novel secretory organelle? Mol Biochem Parasitol 2003;132:17–26.
[6] Kriek N, Tilley L, Horrocks P, Pinches R, Elford BC, Ferguson DJP, et al. Characterization of the pathway for transport of the cytoadherence-mediating protein, PfEMP1, to the host cell surface in malaria parasite-infected erythrocytes. Mol Microbiol 2003;50:1215–27.
[7] Taraschi TF, O'Donnell M, Martinez S, Schneider T, Trelka D, Fowler VM, et al. Generation of an erythrocyte vesicle transport system by *Plasmodium falciparum* malaria parasites. Blood 2003;102:3420–6.
[8] Haldar K, Mohandas N, Samuel BU, Harrison T, Hiller NL, Akompong T, et al. Protein and lipid trafficking induced in erythrocytes infected by malaria parasites. Cell Microbiol 2002;4:383–95.
[9] Saliba KJ, Kirk K. Nutrient acquisition by intracellular apicomplexan parasites: staying in for dinner. Int J Parasitol 2001;31:1321–30.
[10] Sherman IW, Winograd E. Antigens on the *Plasmodium falciparum* infected erythrocyte surface are not parasite derived. Parasitol Today 1990;6:317–20.
[11] Eda S, Sherman IW. Cytoadherence of malaria-infected red blood cells involves exposure of phosphatidylserine. Cell Physiol Biochem 2002;12:373–84.
[12] Hsiao LL, Howard RJ, Aikawa M, Taraschi TF. Modification of host cell membrane lipid composition by the intra-erythrocytic human malaria parasite. Biochem J 1991;274:121–32.
[13] Maguire P, Prudhomme J, Sherman IW. Alterations in erythrocyte membrane phospholipid organization due to the intracellular growth of the malaria parasite *Plasmodium falciparum*. Parasitology 1991;102:179–86.
[14] Maguire PA, Sherman IW. Phospholipid composition, cholesterol content and cholesterol exchange in *Plasmodium falciparum*-infected red cells. Mol Biochem Parasitol 1990;38:105–12.
[15] Nagao E, Seydel KB, Dvorak JA. Detergent-resistant membrane rafts are modified by a *Plasmodium falciparum* infection. Exp Parasitol 2002;102:57–9.
[16] Vial HJ, Eldin P, Tielens AG, van Hellemond JJ. Phospholipids in parasitic protozoa. Mol Biochem Parasitol 2003;126:143–54.
[17] Koontz JL, Marcy JE. Formation of natamycin:cyclodextrin inclusion complexes and their characterization. J Agric Food Chem 2003;51:7106–10.
[18] O'Day DM, Ray WA, Robinson RD, Head WS. Correlation of in vitro and in vivo susceptibility of Candida albicans to amphotericin B and natamycin. Invest Opthalmol Vis Sci 1987;28:596–603.
[19] Teerlink T, De Kruijff B, Demel RA. The action of pimaricin, etruscomycin and amphotericin B on liposomes with varying sterol content. Biochem Biophys Acta 1980;599: 484–92.
[20] Gallis HA, Drew RH, Pickard WW. Amphotericin B: 30 years of clinical experience. Rev Infect Dis 1990; 12:308–29.
[21] Baginski M, Resat H, McCammon JA. Molecular properties of amphotericin B membrane channel: a molecular dynamics simulation. Mol Pharmacol 1997;52: 560–70.
[22] Kleinberg ME, Finkelstein A. Single-length and double-length channels formed by nystatin in lipid bilayer membranes. J Membr Biol 1984;80:257–69.
[23] Volpon L, Lancelin J-M. Solution NMR structure of five representative glycosylated polyene macrolide antibiotics with a sterol-dependent antifungal activity. Eur J Biochem 2002;269:4533–41.
[24] Mehta RT, Hopfer RL, McQueen T, Juliano RL, Lopez-Berestein G. Toxicity and therapeutic effects in mice of liposome-encapsulated nystatin for systemic fungal infections. Antimicrob Agents Chemother 1987;31:1901–3.
[25] Deray G. Amphotericin B nephrotoxicity. J Antimicrob Chemother 2004;49:37–41.
[26] Tiphine M, Letscher-Bru V, Herbrecht R. Amphotericin B and its new formulations: pharmacologic characteristics, clinical efficacy, and tolerability. Transpl Infect Dis 1999;1:273–83.
[27] Hatabu T, Takada T, Taguchi N, Suzuki M, Sato K, Kano S. Potent plasmodicidal activity of a heat-induced reformulation of deoxycholate-amphotericin B (Fungizone) against *Plasmodium falciparum*. Antimicrob Agents Chemother 2005;49:493–6.
[28] Behnke O, Tranum-Jensen J, van Deurs B. Filipin as cholesterol probe. Part II. Filipin-cholesterol interaction in red blood cell membranes. Eur J Cell Biol 1984;35:200–15.
[29] Makler MT, Hinrichs DJ. Measurement of the lactate dehydrogenase activity of *Plasmodium falciparum* as an assessment of parasitemia. Am J Trop Med Hyg 1993;48:205–10.
[30] Ginsburg H, Famin O, Zhang J, Krugliak M. Inhibition of glutathione-dependent degradation of heme by chloroquine and amodiaquine as a possible basis for their antimalarial mode of action. Biochem Pharmacol 1998;56:1305–13.
[31] Kirk K. Membrane transport in the malaria-infected erythrocyte. Physiol Rev 2001;81:495–537.
[32] Glenister FK, Coppel RL, Cowman AF, Mohandas N, Cooke BM. Contribution of parasite proteins to altered mechanical properties of malaria-infected red blood cells. Blood 2002;99:1060–3.
[33] Charbonneau C, Fournier I, Dufresne S, Barwicz J, Tancrède P. The interactions of amphotericin B with various sterols in relation to its possible use in anticancer therapy. Biophys Chem 2001;91:125–33.
[34] Atamna H, Ginsburg H. Origin of reactive oxygen species in erythrocytes infected with *Plasmodium falciparum*. Mol Biochem Parasitol 1993;61:231–41.

[35] Huber SM, Uhlemann A-C, Gamper NL, Duranton C, Kremsner PG, Lang F. *Plasmodium falciparum* activates endogenous Cl^- channels of human erythrocytes by membrane oxidation. EMBO J 2002;21:22–30.
[36] Samuel BU, Mohandas N, Harrison T, McManus H, Rosse W, Reid M, et al. The role of cholesterol and glycosylphosphatidylinositol-anchored proteins of erythrocyte rafts in regulating raft protein content and malarial infection. J Biol Chem 2001;276:29319–2.
[37] Jackson KE, Klonis N, Ferguson DJP, Adisa A, Dogovski C, Tilley L. Food vacuole-associated lipid bodies and heterogeneous lipid environments in the malaria parasite *Plasmodium falciparum*. Mol Microbiol 2004;54:109–22.
[38] Lauer S, VanWye J, Harrison T, McManus H, Samuel BU, Hiller NL, et al. Vacuolar uptake of host components, and a role for cholesterol and sphingomyelin in malarial infection. EMBO J 2000;19:3556–64.